Journal of Alloys and Compounds 495 (2010) 412–416

Contents lists available at ScienceDirect

Journal of Alloys and Compounds

journal homepage: www.elsevier.com/locate/jallcom

High-frequency magnetoimpedance properties in Finemet-type ribbons with a Cu–Co electrodeposited layer

Josefina M. Silveyra[a,*], Marco Coïsson[b], Federica Celegato[b], Paola Tiberto[b], Franco Vinai[b], Javier A. Moya[a], Victoria J. Cremaschi[a]

[a] Lab. de Sólidos Amorfos, INTECIN, FIUBA-CONICET, Paseo Colón 850, (C1063ACV) Buenos Aires, Argentina
[b] INRIM, Strada delle Cacce 91, I-10135 Torino, Italy

ARTICLE INFO

Article history:
Received 9 July 2008
Received in revised form 18 October 2009
Accepted 19 October 2009
Available online 29 October 2009

Keywords:
Amorphous materials
Composite materials
Magnetic measurements

ABSTRACT

A comprehensive analysis of magnetoimpedance phenomena in Finemet-type as spun ribbons with a Cu–Co layer electrodeposited at different currents is presented here as a function of microstructure. The measurements were performed in moderate and high frequencies (30 kHz–6 GHz) under an axial magnetic field, up to 25 kA/m. The magnetoimpedance variations have been studied by measuring the reflection parameter S_{11} of a coaxial line containing the magnetic sample by means of a vector network analyzer.

The GMI *vs* applied field curve does not show a monotonic decay but displays a maximum. GMI first increases with frequencies up to ~10 MHz reaching values of $\Delta Z/Z_{max} \sim 20\%$. At higher frequencies the GMI ratio is seen to decrease becoming vanishingly small at ~1 GHz.

1. Introduction

There is a constant effort in finding new materials with physical properties useful for magnetic sensors. Within this mainframe, the discovery of the giant magnetoimpedance (GMI) effect, large change of impedance in soft magnetic alloys when submitted to an external magnetic field, has opened a new branch in research. The growing number of publications focused on GMI is related to its potential applications. Furthermore, the phenomenon is a powerful tool to investigate intrinsic and extrinsic magnetic properties of soft magnetic materials [1,2].

If a soft magnetic conductor with an applied AC current at frequency (f) is placed in an axial DC magnetic field (H_{DC}), it is possible to observe a variation in the intrinsic impedance of the sample as a function of H_{DC}. This effect, described by the classical theory of electromagnetism, is due to the change of circumferential permeability in wires (μ_ϕ) or transverse permeability in ribbons (μ_t) caused by the axial DC magnetic field [3].

At very low f (up to few kHz), GMI is essentially a magnetoinductive effect [1], but from roughly 10 kHz the dominant effect is the variation of the skin depth δ, *i.e.*, the depth at which the AC current density reduces to 37% of that at the surface [4] and can be written as $\delta = [1/(\pi\sigma\mu f)]^{1/2}$, where σ is the electrical conductivity of the sample and μ is μ_t or μ_ϕ. GMI depends on several factors including H_{DC}, f and amplitude of the AC current flowing through the conductor, sample geometry, composition and microstructure. This is described by the Maxwell equation for the AC magnetic field induced by the excitation current, together with the Landau–Lifshitz–Gilbert rotational equation for the magnetization vector [5]. While these equations are usually nonlinear, the solutions can be substantially simplified if linear approximation is used. In the range of f from 10 kHz to hundreds of MHz both domain wall motion and domain rotation contribute to μ_t, the latter starting to dominate at higher f values. Different theoretical models were employed to understand the influence of each contribution [6]. At even higher f values FMR (ferromagnetic resonance) may occur [1].

It has been shown that amorphous ribbons and wires are good candidates for highly sensitive optimized systems (*i.e.* big variations in the impedance at low H_{DC}); the largest variations have been obtained in samples characterized by a magnetic domain pattern transversal to the alternating current flux. In general, Fe-based alloys have shown to have lower GMI responses than Co-based wires and ribbons. However, higher GMI values comparable to the ones typically measured in Co-based systems have been observed in Fe-based alloys too. The state of art of GMI in soft magnetic materials has recently been reviewed by Knobel *et al.* [3].

GMI measurements have generally been performed up to 10 MHz [7], mainly because at higher f the conventional tech-

* Corresponding author at: Lab. de Sólidos Amorfos, INTECIN, FIUBA-CONICET, Paseo Colón 850, (C1063ACV) Buenos Aires, Argentina. Tel.: +54 11 4343 9891 232; fax: +54 11 4331 1852.
E-mail addresses: jsilveyra@fi.uba.ar, finisilveyra@gmail.com (J.M. Silveyra).

0925-8388/$ – see front matter © 2009 Elsevier B.V. All rights reserved.
doi:10.1016/j.jallcom.2009.10.173

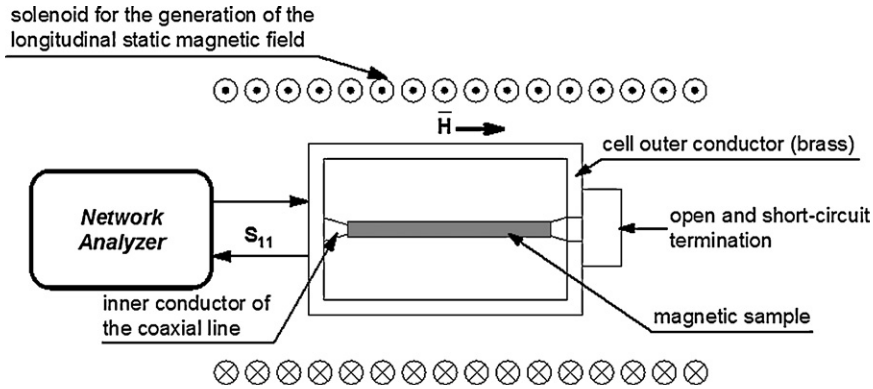

Fig. 1. Schematic representation of the experimental set-up.

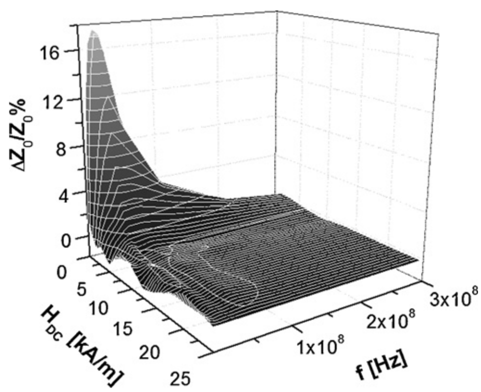

Fig. 2. GMI ($\Delta Z_0/Z_0\%$) *vs* applied field (H_{DC}) and frequency (*f*) for a Finemet-type ribbon with Cu–Co layer deposited with 1.29 mA/cm^2.

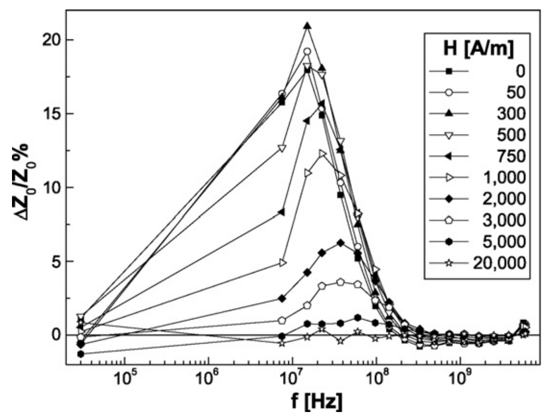

Fig. 4. GMI ($\Delta Z_0/Z_0\%$) *vs* frequency (*f*) for a Finemet-type ribbon with Cu–Co layer deposited with 1.29 mA/cm^2. Each curve corresponds to different applied magnetic fields (H_{DC}). The lines between experimental points are guides for the eyes.

nique (volt-amperometric or four probes) fails. Exhaustive studies have already been performed on Finemets (FeSiBNbCu) ribbons, correlating structure and magnetic properties with GMI measurements, usually up to this frequency [2,8,9]. In fact, in the region of microwave frequencies, it is necessary to revise the definition of magnetoimpedance avoiding the use of voltage and current, which are not always well-defined quantities [10]. The reason is that the wavelength of the signal travelling through the device or circuit is of the same order of magnitude or even shorter than the physical dimensions of the device. Then, a new approach called transmission line theory must be applied instead of circuit theory. An alternative experimental set-up can be used which is based on the concept of scattering *S* parameter and extends GMI characterizations to GHz region [11].

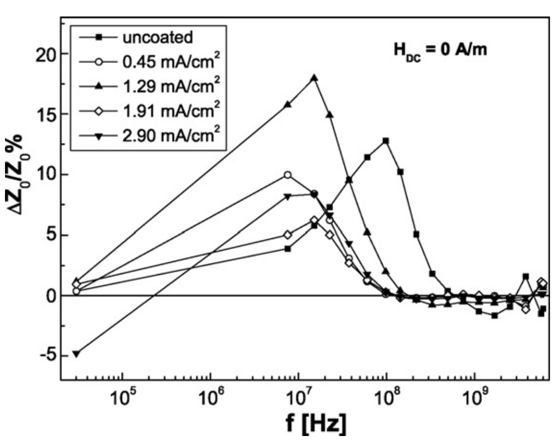

Fig. 3. Zero field GMI ($\Delta Z_0/Z_0\%$) *vs* frequency (*f*) for an uncoated Finemet-type ribbon and with Cu–Co layer deposited with 0.45, 1.29, 1.91 and 2.90 mA/cm^2. The lines between experimental points are guides for the eyes.

A few years ago, a new system has been reported in which Cu–Co thin films were electrodeposited on a Finemet-type ribbon [12]. The giant magnetoresistive effect in these samples was studied in the past [13]. In this work GMI effect at high frequencies is analysed in such a system.

2. Experimental

Finemet-type ribbons ($Fe_{73.5}Si_{6.5}Ge_7B_9Nb_3Cu_1$) [14] ~1 mm wide and ~20 μm thick were produced by the melt-spinning technique with a single wheel on air. They were mechanically polished using 2000 and 4000 emery papers on both surfaces and subsequently annealed in vacuum for 30 min at 573 K to release stresses. Afterwards, a granular Cu–Co layer was electrodeposited in galvanostatic mode. Several samples were electroplated with different current density values applied with a potensiostat/galvanostat during 15 min. The electrolytic solution was prepared using distilled water with $CoSO_4{\cdot}7H_2O$, $CuSO_4{\cdot}5H_2O$, $Na_3C_6H_5O_7{\cdot}2H_2O$, NaCl and HCl; NaOH and HCl were used for regulating the pH up to 6 [13]. A stainless steel tube was used as anode and the ribbon (*i.e.* the cathode) was placed in its centre. This shape was chosen in order to achieve a homogeneous electrostatic field and therefore a homogeneous electrodeposition. Electrodes were cleaned for 5 min in an ultrasonic cleaner with acetone followed by an isopropylic bath before each experiment. The electrodeposition was performed on air, under magnetic stirring at a temperature of 308 K controlled by a closed heating system with a water jacket.

High-frequency impedance measurements were carried out with a vector network analyser at room temperature. The set-up is described by Brunetti *et al.* [11]. The sample, ~13 mm long, is glued with silver paste and constitutes the inner conductor of a coaxial line; the brass holder is the outer one. A longitudinal H_{DC} is applied by means of a solenoid as shown in Fig. 1. The network analyser applies an electromagnetic wave in TEM mode (transverse electromagnetic transmission) and measures the reflection *S*-parameters, which are used to calculate the characteristic impedance Z_0 of the line. Z_0 is the impedance the line would have if it were of infinite length and gives comparable results with those that can be obtained from conventional measurements at low frequency. The total impedance connected to

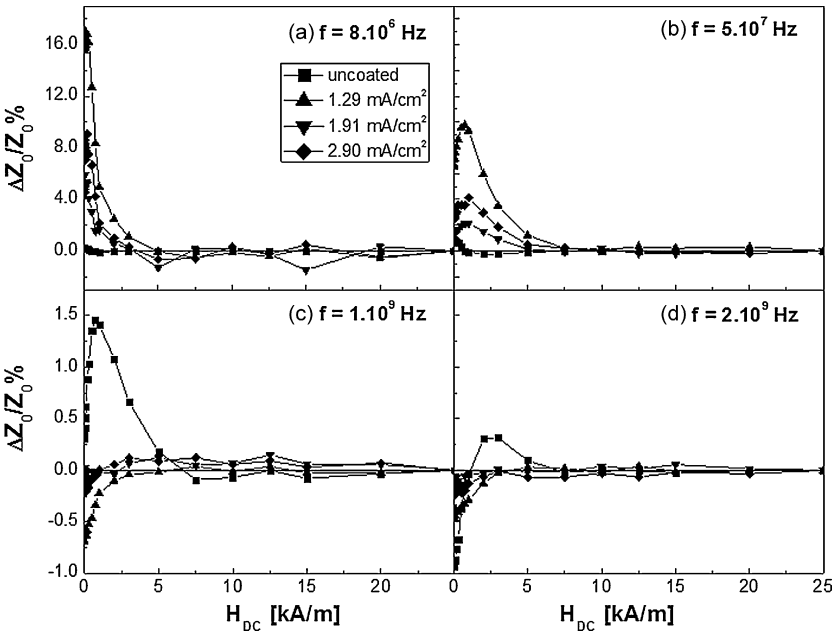

Fig. 5. GMI ($\Delta Z_0/Z_0$%) *vs* applied field (H_{DC}) at different frequencies (*f*), for an uncoated Finemet-type ribbon and one with Cu–Co layer deposited with 1.29, 1.91 and 2.90 mA/cm^2: (a) *f* = 3.104 Hz, (b) *f* = 5.107 Hz, (c) *f* = 1.109 Hz and (d) *f* = 2.109 Hz. The lines between experimental points are guides for the eyes.

the network analyzer port is not only a function of the magnetic properties of the studied material, but also of the termination applied to the line. However, if a suitable procedure is applied to extract the characteristic impedance Z_0 from the total impedance data, thus getting rid of the contribution of the termination applied to the line, a magnetoimpedance determination that is comparable to the conventional volt-amperometric one can be obtained [11]. The GMI value is defined as: $\Delta Z_0/Z_0\% = [Z_0(H) - Z_0(H_{max})]/Z_0(H_{max}) \times 100$. H_{DC} interval was 0–25 kA/m and frequency *f* ranged from 30 kHz to 6 GHz. Magnetoimpedance variation is reported versus H_{DC} and *f*.

Hysteresis loops were measured with a VSM (vibrating sample magnetometer) under an applied maximum magnetic field of 80 kA/m in the ribbon plane in longitudinal and transversal directions. From these curves saturation (mass) magnetization (σ_S) was obtained. Out-of-plane magnetic domains were observed by AFM/MFM imaging (atomic force microscopy/magnetic force microscopy).

3. Results and discussion

An overall picture of GMI dependence on H_{DC} and *f* is reported in Fig. 2.

As shown in Fig. 3, GMI has non-monotonic frequency dependence. In particular, the following features are observed:

(i) For frequencies lower than 100 kHz the GMI response, attributed to magnetoinductive effect, is negligible. This is because δ is larger than the thickness of the ribbon and the current flows through the entire cross-section [4].

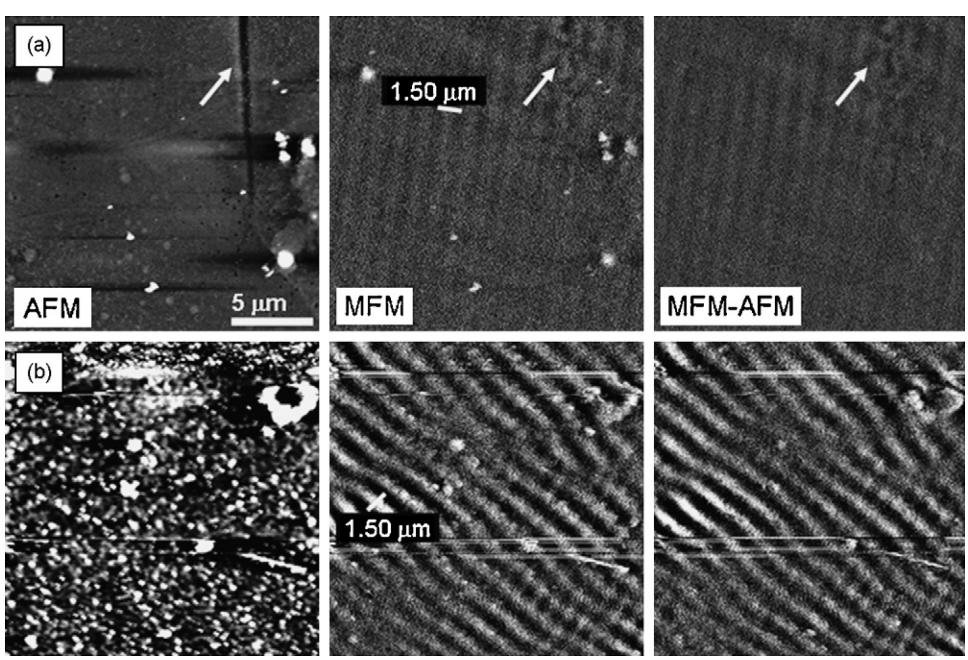

Fig. 6. AFM, MFM and subtracted images of (a) for an uncoated Finemet-type sample and (b) a sample with Cu–Co layer deposited with 1.29 mA/cm^2. Domain period (~1.5 mm) and its inhomogeneity due to defects on the ribbon are marked.

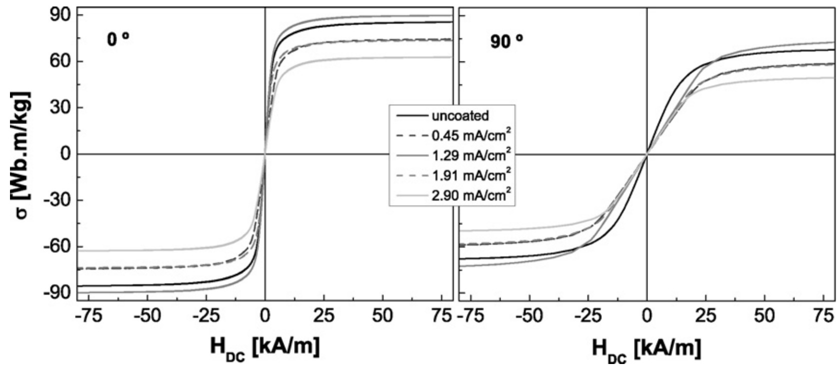

Fig. 7. Mass magnetization (σ) *vs* applied field (H_{DC}): 0° along ribbon's longitudinal axis (left) and 90° along transversal axis (right).

(ii) For frequencies higher than 100 kHz and up to a few hundred of MHz, GMI rapidly increases, reaching a maximum ratio at a certain critical frequency f_c. As frequency rises, δ decreases becoming comparable to the ribbon thickness, thus zero field impedance strongly increases. The maximum value achieved depends on several factors such as temperature, geometry, anisotropy, stresses and sample composition.

(iii) At high frequencies magnetic permeability relaxes since domains rotation starts prevailing over domain wall movement on the magnetization process. Thus, the product $\mu_t.\,f$ decreases and as a result δ increases. Hence, the GMI response is again vanishingly small, sometimes reaching even negative values [15].

(iv) At 4 GHz there is an asymptotic trend due to the resonance of the measurement cell itself. No ferromagnetic resonance phenomenon is observed.

The application of H_{DC} along the ribbon axis decreases the μ_t; δ becomes comparable to the ribbon thickness at higher frequencies, resulting in a shift of f_c [4]. However, the GMI maximum value is reduced (Fig. 4). Nevertheless, when H_{DC} is increased up to 300 A/m, GMI maximum value increases, as will be discussed later on GMI *vs* H_{DC} response (Fig. 5(b)–(d)). Notice that in spite of the shift, all the curves remain "inside" the larger one that acts as an envelope limiting their possible GMI and f_c values, a fact that was not considered in previous publications.

Comparing Cu–Co coated samples with the not deposited one, it is seen that f_c shifts towards lower values as it was observed in other composite samples with ferromagnetic or conductive layers [16]. The reason why in some samples the shift is larger than in others and why the maximum GMI obtained has different values is not yet understood since there are many parameters which vary with current density, influencing the effect in different ways: stresses induced in the electrodeposition process, conductivity, permeability and thickness of the coating.

GMI response *vs* H_{DC}, can be seen in Fig. 5. Only results obtained for positive applied fields are shown since MI curves are symmetric with respect to the magnetic field and are not hysteretic. This is a usual feature of MI for amorphous wires and ribbons [7]. On the evolution towards higher frequencies it was seen: at low-medium frequencies (Fig. 5(a)) all ribbons have monotonous behaviour, indicating that the main magnetization process that takes place is attributed to domain wall displacement [6]. When the frequency is raised, a peak appears since domain rotation process starts to prevail over domain wall movement (Fig. 5(b)–(d)). However, this magnetization process transition takes place at lower frequencies in samples with Cu–Co layer than in Finemet-type ribbons. In the end, GMI is vanishingly small in all samples, even negative at certain applied fields in agreement with GMI *vs f* response [15] (Fig. 3).

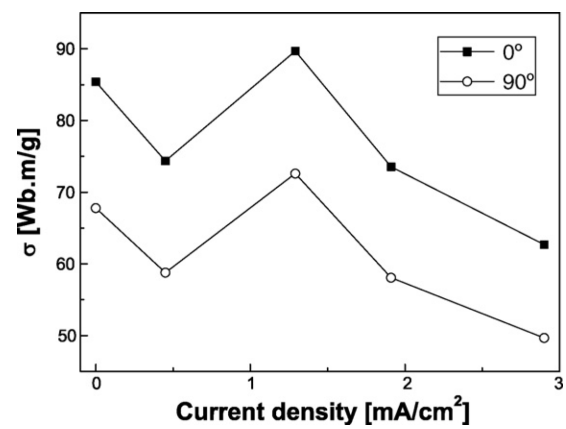

Fig. 8. Saturation (mass) magnetization (σ_s) *vs* current density applied on the electrodeposition.

Domain structures were observed by means of MFM. In Fig. 6 stripe out-of-plane domain patterns (~1.5 μm width) on the ribbons with and without Cu–Co layer can be seen. As there is no difference between them, we conclude that the pattern corresponds to the base ribbon (Finemet). It can also be seen that the domains are not uniform. This is caused by stress inhomogeneity and defects in the sample.

Hysteresis loops measured in longitudinal and transversal directions are shown in Fig. 7. The dependence of saturation (mass) magnetization (σ_S = magnetic moment/total mass) with the electrodeposition current density is plotted in Fig. 8 and can be explained as follows: when Cu–Co is deposited the total mass that divides the magnetic moment increases linearly with current density, while the amount of Co (ferromagnetic) does exponentially. As a result, for low current densities, mass effect dominates over the magnetic contribution of Co, decreasing σ_S (Wb m/kg). At intermediate current densities, the ferromagnetic contribution of Co raises the total σ_S up to a maximum value, but at higher *f* Cu–Co mass starts lowering σ_S again.

4. Conclusions

A comprehensive analysis of magnetoimpedance phenomena at high frequencies in such arrangement was presented here for extending the knowledge on composite samples. As the magnetic permeability was affected by anisotropies and stresses (induced during the sample preparation or during the measurement), the impedance variation reflected structural and magnetic properties of the material. A value of $\Delta Z/Z_{max}$ ~ 20% was measured on the ribbon with Cu–Co layer deposited with 1.29 mA/cm^2. By means of GMI responses dominating magnetization processes in samples with and without electroplated Cu–Co layer were identified at different H_{DC} and f values. They were in essence the expected ones for amorphous materials. Out-of-plane domain patterns did not seem to vary after Cu–Co deposit. As a consequence, the domain patterns observed by MFM correspond to the Finemet-type ribbon. On the other hand, it was explained how the coating changed σ_S and created a longitudinal anisotropy almost independently of the applied current density. This can be observed from the tilt of the slope of the transversal hysteresis loops after the deposition.

References

[1] F. Vinai, M. Coïsson, P. Tiberto, J. Magn. Magn. Mater. 300 (2006) e82–e87.
[2] V.M. Prida, P. Gorría, G.V. Kurlyandskaya, M.L. Sánchez, B. Hernando, M. Tejedor, Nanotechnology 14 (2003) 231–238.
[3] M. Knobel, M. Vázquez, L. Kraus, Handbook Magn. Mater. 15 (2003) 497–563.
[4] P. Jantaratana, C. Sirisathitkul, IEEE Trans. Magn. 42 (2006) 358–362.
[5] L.D. Landau, E.M. Lifshitz, Electrodynamics of Continuous Media, 2nd ed., Pergamon, NY, 1984.
[6] K.-S. Byon, S.-C. Yu, J.S. Kim, C.G. Kim, IEEE Trans. Magn. 36 (2000) 3439–3441.
[7] L.V. Panina, K. Mohri, K. Bushida, M. Noda, J. Appl. Phys. 76 (1994) 6198–6203.
[8] M. Tejedor, B. Hernando, M.L. Sánchez, V.M. Prida, J.M. García-Beneytez, M. Vázquez, G. Herzer, J. Magn. Magn. Mater. 185 (1998) 61–65.
[9] P. Gorria, V.M. Prida, M. Tejedor, B. Hernando, M.L. Sánchez, Physica B 299 (2001) 215–224.
[10] J.D. Kraus, Electromagnetics, Mc Graw-Hill, New York, 1991, pp. 460–470.
[11] L. Brunetti, M. Coïsson, P. Tiberto, F. Vinai, J. Magn. Magn. Mater. 249 (2002) 310–314.
[12] J.H. Min, J.-H. Wu, J.U. Cho, Q.X. Liu, J.H. Lee, Y.-D. Ko, J.-S. Chung, J.-H. Lee, Y.K. Kim, J. Magn. Magn. Mater. 404 (2006) e100–e102.
[13] J.M. Silveyra, V.J. Cremaschi, J.A. Moya, H.R.M. Sirkin, Cintas tipo Finemet con capa Cu–Co electrodepositada presentan GMR, 92° Reunión Nacional de la Asociación Física Argentina (2007).
[14] J.A. Moya, V.J. Cremaschi, H. Sirkin, Phys. B: Condes. Mater. 389 (2007) 159–162.
[15] L. Brunetti, M. Coïsson, P. Tiberto, F. Vinai, H. Chiriac, F. Borza, Sens. Actuators 91 (2001) 203–206.
[16] R.L. Wang, Z.J. Zhao, L.P. Liu, W.Z. Yuan, X.L. Yang, J. Magn. Magn. Mater. 285 (2005) 55–59.